JOURNAL OF MOLECULAR SPECTROSCOPY 161, 186–207 (1993)

Fourfold Clusters of Rovibrational Energy Levels in the Fundamental Vibrational States of H_2Se

IGOR N. KOZIN* AND PER JENSEN†[1]

*Physikalisch-Chemisches Institut, Justus-Liebig-Universität Giessen, Heinrich-Buff-Ring 58, W-6300 Giessen, Germany; and †FB 9-Theoretische Chemie, Bergische Universität-Gesamthochschule Wuppertal, Gaussstrasse 20, W-5600 Wuppertal 1, Germany

We report here a calculation of the rotation–vibration energies in the ν_1, ν_2, ν_3, and $2\nu_2$ vibrational states of $H_2{}^{80}Se$ using the MORBID (Morse oscillator rigid bender internal dynamics) Hamiltonian and computer program [P. Jensen, *J. Mol. Spectrosc.* **128,** 478–501 (1988); *J. Chem. Soc. Faraday Trans. 2* **84,** 1315–1340 (1988)]. As input data for the calculation, we employ a potential energy surface recently determined from experimental data by means of the MORBID approach [P. Jensen and I. N. Kozin, *J. Mol. Spectrosc.*, in press.]. For all of the vibrational states considered, the calculation shows that as J increases, fourfold rovibrational energy clusters are formed. This effect has already been experimentally verified for the vibrational ground state and its origin was shown to lie in the centrifugal distortion of the molecule [I. N. Kozin, S. P. Belov, O. L. Polyansky, and M. Yu. Tretyakov, *J. Mol. Spectrosc.* **152,** 13–28 (1992); I. N. Kozin, O. L. Polyansky, S. I. Pripolzin, and V. L. Vaks, *J. Mol. Spectrosc.* **156,** 504–506 (1992); I. N. Kozin, S. Klee, P. Jensen, O. L. Polyansky, and I. M. Pavlichenkov, *J. Mol. Spectrosc.*, **158,** 409–422 (1993)]. We find here that the cluster formation in the ν_2 and $2\nu_2$ vibrational states is completely analogous to that in the vibrational ground state. For the ν_1/ν_3 interacting vibrational states, however, we predict a new type of fourfold clusters. We can describe their formation as a coalescence (with increasing J) of two energy doublets, where one doublet belongs to the ν_1 vibrational state and the other one to the ν_3 vibrational state. An interpretation of the "new" cluster eigenstates is given, and the origins of the cluster formation are discussed in terms of semiclassical theory. The semiclassical analysis shows that the new clusters are caused essentially by the rotational interactions between the ν_1 and the ν_3 states. The predicted term values from the present work are found to be in good agreement with experimental values from a very recent study by J.-M. Flaud, C. Camy-Peyret, H. Bürger, and H. Willner, *J. Mol. Spectrosc.* **161,** 157–169 (1993). However, the available experimental data do not extend to sufficiently high J and K values to allow an experimental verification of the existence of the new clusters.

I. INTRODUCTION

Recent experimental studies (*1–3*) have provided conclusive evidence for the formation of nearly degenerate, four-member groups of rotational energy levels in the vibrational ground state of the H_2Se molecule. This effect was first predicted for the vibrational ground state of H_2O on the basis of semiclassical theory and model quantum mechanical calculations (*4–7*). However, for H_2O the fourfold clusters are found for J and K values so high that the transitions involving the cluster states are too weak to be observed experimentally at the present time. In the vibrational ground state of H_2Se, the cluster structure of the rotational energy levels becomes apparent already for $J \leqslant 20$, and in Refs. (*1–3*) the existence of the clusters could be unambiguously established through the observation of rotational transitions involving $J \leqslant 23$.

[1] Guest professor, 1992–93. On leave from Physikalisch-Chemisches Institut, Justus-Liebig-Universität Giessen, Heinrich-Buff-Ring 58, W-6300 Giessen, Germany.

0022-2852/93 $5.00

In a recent paper (*8*) we reported the determination of the potential energy surface for the electronic ground state of the hydrogen selenide molecule by a direct least-squares fitting to experimental data involving $J \leq 5$ using the MORBID (Morse oscillator rigid bender internal dynamics) approach (*9–11*). With the resulting potential energy function we predicted the rotational energy level structures in the vibrational ground states of H_2Se and D_2Se up to $J = 40$. Even though the fitted data involved $J \leq 5$ only, so that the fitted energy spacings were highly similar to those of a rigid asymmetric rotor with the equilibrium rotational constants of H_2Se, our calculation of the cluster structure in the vibrational ground state of $H_2{}^{80}Se$, which has been experimentally observed up to $J = 23$ (*1–3*), was in good agreement with the experimental results [see Fig. 2 of Ref. (*8*)].

In the present work we analyze the cluster formation in the three fundamental vibrational states and in the $2\nu_2$ state (which is close to the ν_1 and ν_3 states) of H_2Se through a MORBID calculation using the fitted potential energy function from Ref. (*8*). We find that the cluster formation in the ν_2 and $2\nu_2$ vibrational states involves the centrifugal distortion mechanism already discussed for the vibrational ground state in Refs. (*1–8*). However, for the ν_1/ν_3 interacting vibrational states we find that fourfold clusters arise through coalescence (with increasing J) of energy doublets belonging to the ν_1 vibrational state with doublets belonging to the ν_3 state. The wavefunctions of the cluster states are fifty-fifty mixtures of ν_1 and ν_3 basis states. The formation of these "new" clusters involves a mechanism different from that responsible for the fourfold clusters in the vibrational ground state and in the ν_2 and $2\nu_2$ states. The ν_1/ν_3 clusters are mainly caused by the interaction between the ν_1 and ν_3 vibrational states. The rotation–vibration motion in the "new" cluster states is interpreted through an analysis of the cluster wavefunctions, and a discussion of the cluster formation in terms of semiclassical theory is presented.

II. THE CALCULATION

In the present work, we take the potential energy function for the electronic ground state of H_2Se to be given by the analytical expression defined by Eqs. (1)–(5) of Ref. (*8*). The values of the parameters in the expression are taken from Table II of Ref. (*8*). These values were optimized in a least-squares fitting (using the MORBID program) to an extensive set of rotation–vibration energy spacings for $H_2{}^{80}Se$ and its isotopic species. The input data consisted of 303 experimental energy separations involving rotation–vibration energy levels with $J \leq 5$ belonging to the three isotopically substituted molecules $H_2{}^{80}Se$, $D_2{}^{80}Se$, and $HD^{80}Se$.

The calculation reported here was carried out with the MORBID Hamiltonian and computer program (*9–11*) using the potential energy function described above. The MORBID approach treats the complete rotational and vibrational motion of a triatomic molecule and calculates the eigenvalues of the rotation–vibration Hamiltonian variationally, i.e., without the use of perturbation theory. Extensive descriptions of the MORBID approach are given in Refs. (*9–11*), and Ref. (*8*) gives a summary.

The MORBID program represents the rotation–vibration wavefunctions as linear combinations of basis functions $|N_{\text{vib}}\Gamma_{\text{Sym}}\rangle|v_2, K\rangle|J, K, M, \tau\rangle (K \geq 0)$, where $|N_{\text{vib}}\Gamma_{\text{Sym}}\rangle$ is a stretching basis function, obtained as eigenfunctions of the Hamiltonian $\hat{H}_{\text{Stretch}}$ [Eq. (58) of Ref. (*9*)] which describes the molecule as stretching with its bond angle fixed at the equilibrium value α_e. The index N_{vib} characterizes the zeroth order stretching state, and Γ_{Sym} is the irreducible representation spanned by the function $|N_{\text{vib}}\Gamma_{\text{Sym}}\rangle$ in the appropriate molecular symmetry group. The factor function $|v_2,$

$K\rangle$ [see Section V of Ref. (*9*)] is an eigenfunction for the Hamiltonian $\hat{H}_{\text{Bend}}$ [Eq. (63) of Ref. (*9*)] describing the molecule as bending and rotating around the molecule-fixed z-axis (see Fig. 1) with its bond lengths fixed at the equilibrium values r_1^e and r_3^e. The quantity v_2 is the bending quantum number for a bent triatomic molecule and K is the rotational quantum number describing rotation around the molecule-fixed z-axis (Fig. 1). Finally, the factor function $|J, K, M, \tau\rangle$ is a symmetrized rigid-rotor eigenfunction defined by Eq. (7.1) of Ref. (*12*).

We have calculated the rotation–vibration energy levels of $H_2{}^{80}Se$ for $J = 0$ through 40 in the vibrational ground state, in the v_2 state, and in the heavily interacting "triad" of states $v_1/v_3/2v_2$. The results for the vibrational ground state were already given in Ref. (*8*), so in the present work we report the calculated energy level structures for the excited vibrational states only. The calculation was done with a basis set in which the stretching problem was prediagonalized [see Ref. (*9*)] with Morse oscillator functions $|n_1 n_3\rangle$ having $n_1 + n_3 \leq 7$. In constructing the final rotation–vibration matrices we used the seven lowest bending basis functions, the six lowest stretching basis functions of A_1 symmetry, and the four lowest stretching basis functions of B_2 symmetry.

Since in the present work we are mainly concerned with cluster formation in the excited vibrational states of $H_2{}^{80}Se$, we do not give lengthy tables of term values. The results are presented graphically in order to make the cluster structure apparent. However, all results from the calculation described here, as well as the results of calculations for other isotopic species of H_2Se, are available from the authors on request.

III. THE v_2 STATE

The rotational energy level manifold in the v_2 vibrational state of $H_2{}^{80}Se$ is shown in Fig. 2 for $J \leq 40$. In the figure, the term values are plotted relative to the highest term value for each J multiplet, and the values calculated by the MORBID program are given as horizontal lines. The empty circles show experimentally derived term values (kindly made available to us prior to publication by J.-M. Flaud and H. Bürger) from the very recent FT-IR study by Flaud *et al.* (*13*); these results became available after we had completed the work reported in Ref. (*8*). Flaud *et al.* (*13*) have obtained

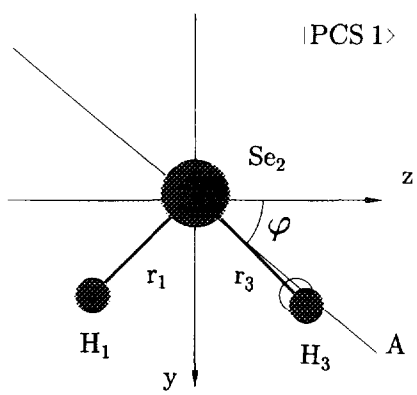

FIG. 1. The numbering of the nuclei and the molecule fixed coordinate system used to describe the H_2Se molecule in the MORBID approach. The molecule fixed x-axis is perpendicular to the plane of the molecule. The figure further shows the localization axis A appropriate for the primitive cluster state $|\text{PCS } 1\rangle$ belonging to the cluster with highest energy in a J multiplet of the v_1/v_3 vibrational state. The axis A forms the angle φ with the molecule fixed z-axis. The excitation of the r_3 stretching found in the state $|\text{PCS } 1\rangle$ is indicated.

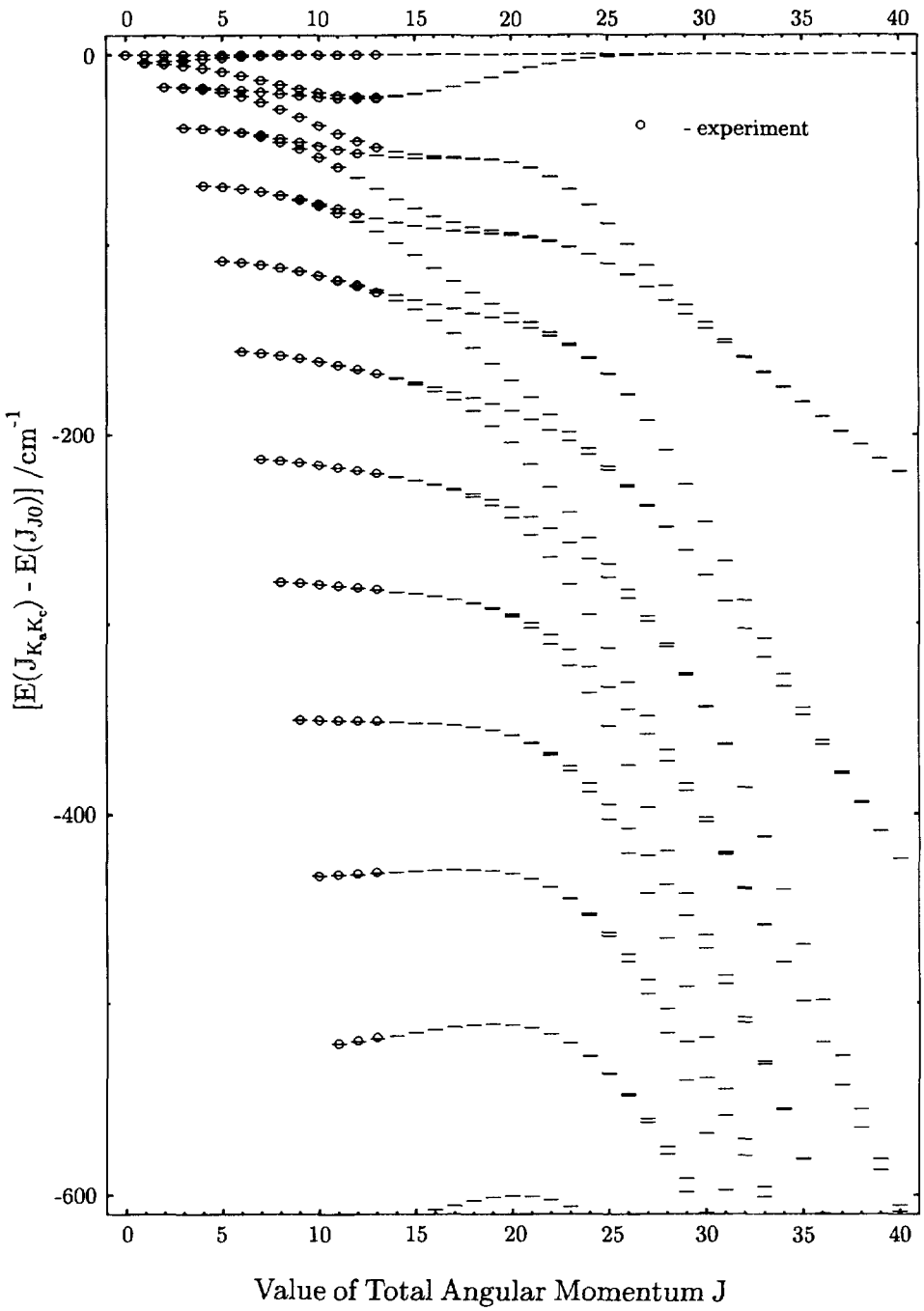

FIG. 2. The rotational energy level structure in the ν_2 vibrational state of $H_2{}^{80}Se$. Term values are plotted relative to the highest term value for each J multiplet, and the values calculated by the MORBID program [using the parameters from Table II of Ref. (*8*)] are given as horizontal lines. The empty circles show experimentally derived term values from the very recent FT-IR study by Flaud *et al.* (*13*).

ν_2 term values for $J \leq 20$. However, the highest term value $E(J_{J0})$ (which we use as energy zero in Fig. 2) has been determined for $J = 0$ through 13, and consequently we display the experimental results for this range of J values only.

Figure 2 shows that as J increases, the 4 highest energies in each J multiplet initially form two doublets, in agreement with the predictions from rigid-rotor theory. However, from $J \approx 12$ the energy difference between the two doublets decreases with increasing J, and for high J values it tends toward zero so that fourfold clusters are formed. At $J > 29$ the energy splittings between the four nearly degenerate states are not visible on the scale of Fig. 2. As J increases further, more fourfold clusters are formed in the J multiplets. At $J > 35$, the 8 highest energies in each J multiplet form two fourfold clusters, and the energy difference between the two clusters increases linearly with J. Finally, at $J = 40$ the 12 highest energies in the J multiplet form three fourfold clusters.

The cluster formation displayed in Fig. 2 is similar to that exhibited by the rotational energy levels in the vibrational ground state of $H_2{}^{80}Se$. Comparison with Fig. 2 of Ref. (*8*), which is an analogous diagram for the vibrational ground state, shows that there is no qualitative change in the cluster formation upon excitation of the bending mode. The rotation–vibration wavefunctions corresponding to the fourfold energy clusters exhibit strong rotational localization. This phenomenon was discussed at considerable length in Ref. (*8*), and we give only a short summary here: We can neglect the small energy splittings between the individual states in a fourfold cluster so that we consider the four cluster states as being exactly degenerate. In this case the cluster corresponds to a four-dimensional space of degenerate eigenfunctions for the rotation–vibration Hamiltonian. One possible set of basis vectors in this space consists of the four eigenfunctions obtained directly in the MORBID calculation. Each of these four eigenfunctions transforms according to one of the irreducible representations A_1, A_2, B_1, and B_2 of the molecular symmetry group of H_2Se, $C_{2v}(M)$ (*14*). However, we showed in Ref. (*8*) that there exists another possible choice of basis vectors in the four-dimensional space of degenerate eigenfunctions, the so-called localized functions suggested by semiclassical theory. These functions are obtained from the MORBID eigenfunctions through a unitary transformation (a rotation in the four-dimensional eigenfunction space); they are not symmetrized in $C_{2v}(M)$. In the present work, we refer to the localized functions as *primitive cluster functions* or *primitive cluster states* (PCS). Of the four primitive cluster functions, two have angular momentum projections of $-\hbar J$ and $\hbar J$, respectively, along an axis A which lies approximately along one of the H–Se bonds (see Fig. 1). When these two functions are subjected to a rotation around the C_2 symmetry axis of the molecule in its equilibrium configuration, we obtain the two remaining primitive cluster functions. Consequently, the two latter functions will have angular momentum projections of $-\hbar J$ and $\hbar J$, respectively, along an axis A' which can be obtained by subjecting A to the C_2 rotation.

IV. THE ν_1, ν_3, AND $2\nu_2$ STATES

Figure 3 gives an overview of the rotation–vibration term values calculated for $H_2{}^{80}Se$ in the $\nu_1/\nu_3/2\nu_2$ region for $J \leq 35$. The three energies present for $J = 0$ are the ν_3 (at 2358 cm^{-1}), ν_1 (at 2344 cm^{-1}), and $2\nu_2$ (at 2060 cm^{-1}) levels. We plot the energies relative to $E_{max}(J)$ defined as the highest energy in each J multiplet of the $\nu_1/\nu_3/2\nu_2$ manifold. Clearly there are many rotation–vibration states in this part of the energy spectrum, and Fig. 3 initially seems somewhat confusing. The fundamental energies of ν_1 and ν_3 differ only by 14 cm^{-1}, so there is significant interaction between

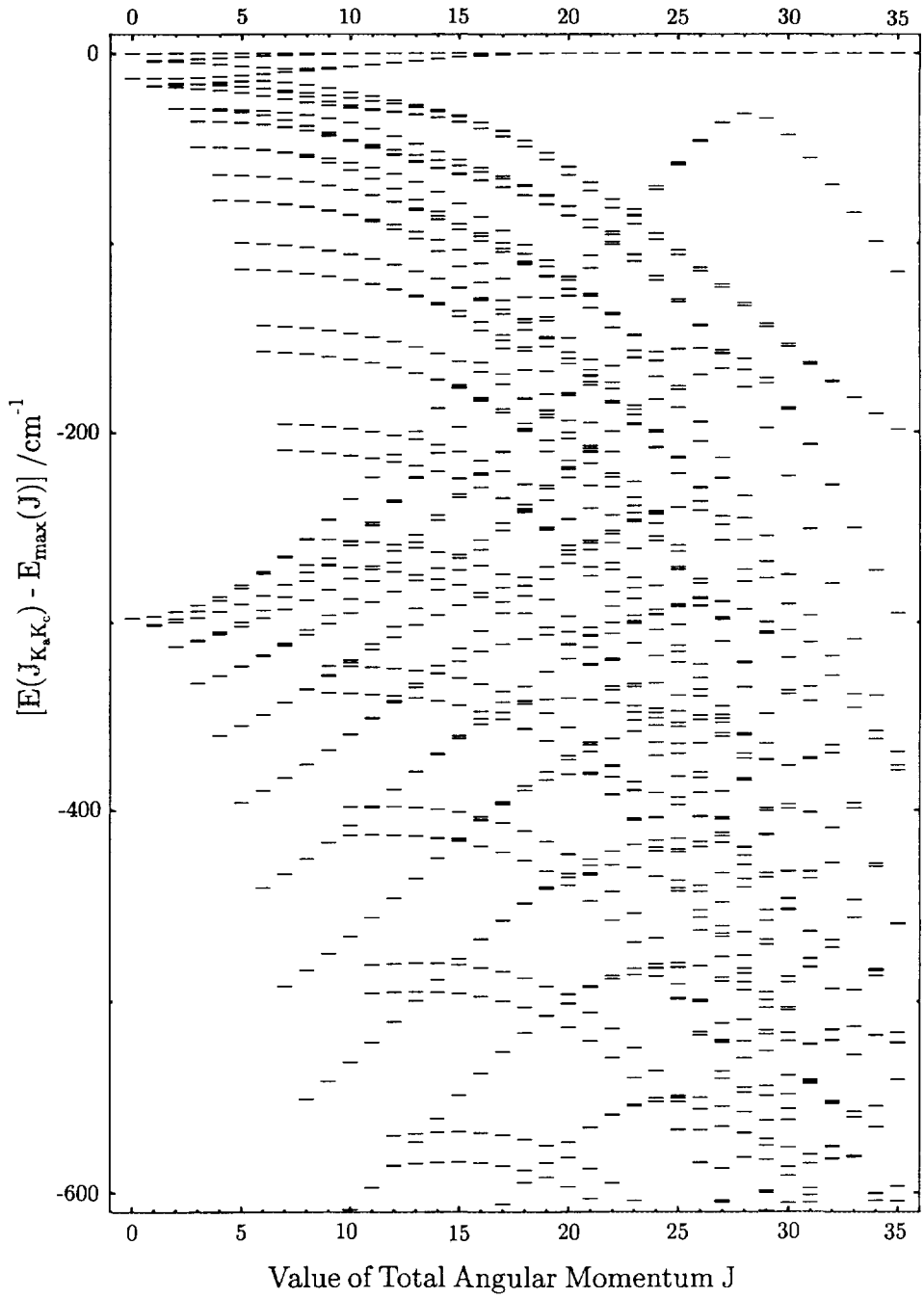

FIG. 3. An overview of the rotation–vibration term values calculated for $H_2{}^{80}Se$ in the $\nu_1/\nu_3/2\nu_2$ region. The three states present for $J = 0$ are the ν_3 (at 2358 cm^{-1}), ν_1 (at 2344 cm^{-1}), and $2\nu_2$ (at 2060 cm^{-1}) levels, respectively.

these two states. It is shown in Ref. (*13*) that in the language of the customary approach to rotation–vibration theory (*15*), this interaction has significant contributions from the Coriolis operator $(Q_1\hat{P}_3 - Q_3\hat{P}_1)\hat{J}_x$ [where Q_i is the normal coordinate associated with the ith normal mode, $\hat{P}_i$ is its conjugate momentum, and $\hat{J}_\alpha$ is the component of the total angular momentum along the molecule-fixed α-axis (Fig. 1)] and from the operator $Q_1Q_3(\hat{J}_y\hat{J}_z + \hat{J}_z\hat{J}_y)$. The interaction originating in the latter operator may be termed a *Birss resonance* (*16*). Further, $2\nu_2$ interacts with ν_1 through a Fermi resonance and with ν_3 through a Coriolis-type resonance. These interactions often lead to such heavy mixing that the assignment of the "standard" harmonic oscillator quantum numbers (v_1, v_2, v_3) to the calculated energy levels becomes rather arbitrary. However, a closer inspection of Fig. 3 reveals that the energy levels show interesting cluster patterns. For example, removing the ν_1 and ν_3 states we find that the energy levels belonging to $2\nu_2$ form fourfold clusters in exactly the same way that we described for the ν_2 state in the preceding section (see Fig. 2). These clusters can still be seen in Fig. 3, but the regular pattern found for the ν_2 state (Fig. 2) is often distorted by local interactions with ν_1 and ν_3.

The most remarkable feature of the term value diagram in Fig. 3 is connected with the fourfold clusters formed by the ν_1/ν_3 levels themselves. This effect is most easily visible in the upper part of the term value diagram and can be observed in Fig. 4a which is an enlargement of the upper 50 cm^{-1} of Fig. 3. For each energy level, we give the vibrational assignment provided by the MORBID program. These assignments are obtained as the vibrational quantum numbers for the basis function with the largest coefficient in the expansion for the MORBID wavefunction given by Eq. (1) (see below). Figure 4a shows that at $J \geqslant 19$, the four highest energies in each J multiplet of the ν_1/ν_3 manifold form a fourfold cluster. It is remarkable, however, that of the two energy doublets merging to form this cluster, one belongs to the ν_1 vibrational state and the other one to the ν_3 vibrational state. For $19 \leqslant J \leqslant 28$, the cluster states are given in Fig. 4a as belonging to ν_3, indicating that ν_3 basis functions provide the largest contribution to the eigenfunctions. However, the contribution from ν_3 is only slightly larger than that from ν_1. As J increases, the cluster wavefunctions smoothly approach fifty-fifty mixtures of ν_1 and ν_3. At $J = 29$, the "top" cluster of the ν_1/ν_3 states undergoes an avoided crossing with the top cluster from the $2\nu_2$ state, and the assignment changes to $2\nu_2$. The partner states in the avoided crossing can be seen in Fig. 3 and, for $26 \leqslant J \leqslant 30$, in Fig. 4a. It is interesting that the clusters are not split by the interaction taking place at the avoided crossing. Obviously, each component of the ν_1/ν_3 cluster interacts with one partner state (of the same symmetry) in the $2\nu_2$ cluster, and the four components are shifted by the same amount through the interactions with their respective partner states. For $J > 35$ (not shown) there is increasingly stronger mixing between basis states. This mixing is necessary to account for the considerable centrifugal distortion in these states, and it leads to the assignment of the top cluster states changing again from $2\nu_2$ to $3\nu_2$.

Figures 3 and 4a show that with increasing J, more fourfold clusters are formed through coalescence of ν_1 and ν_3 levels. For example, in Fig. 4a we see the start of the formation of a second cluster consisting of two ν_1 states and two ν_3 states. For $J > 19$, the corresponding term values are no longer shown in Fig. 4a, but we can follow the progression further in Fig. 3 and find that around $J = 32$, the energy splittings between the individual cluster states are no longer visible on the scale of Fig. 3.

In Ref. (*8*) and in Section III of the present paper, we have discussed the fourfold clusters formed in the vibrational ground state and in the ν_2 state, respectively, of

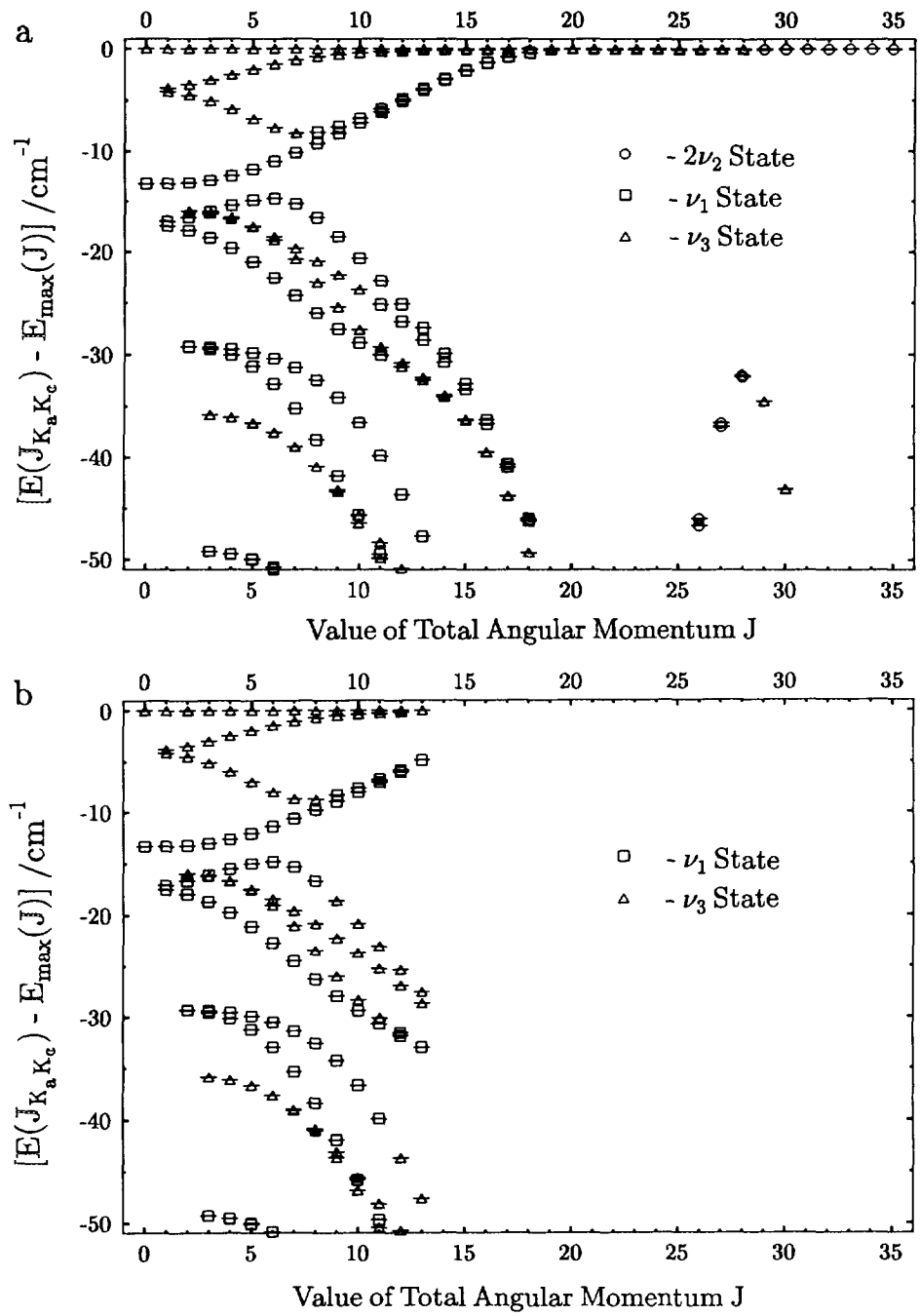

FIG. 4. (a) An enlargement of the upper 50 cm^{-1} of Fig. 3. For each energy level, we give the vibrational assignment provided by the MORBID program. These assignments are obtained as the vibrational quantum numbers for the basis function with the largest coefficient in the expansion for the MORBID wavefunction given by Eq. (1). (b) A term level diagram analogous to Fig. 4a but drawn on the basis of experimentally determined term values and vibrational assignments from Flaud *et al.* (*13*).

$H_2{}^{80}Se$. In both cases, the cluster states involve only one, relatively isolated vibrational state. In the ν_1/ν_3 region we have obviously encountered a new and initially unexpected type of fourfold cluster formed by coalescence of rotation–vibration energy levels belonging to two different vibrational states, ν_1 and ν_3, with different symmetries. For example, if we want to assign "standard" quantum numbers to the cluster states in the top cluster of the ν_1/ν_3 state, we would have to say that the cluster consists of the J_{J0} and J_{J1} levels in the ν_1 state and the J_{J0} and J_{J1} levels of the ν_3 state. We analyze the molecular rotation–vibration motion in the new type of cluster states below.

Figure 4b shows a term value diagram analogous to Fig. 4a but drawn on the basis of experimentally determined term values from Flaud *et al.* (*13*). The figure also shows the vibrational assignments given by these authors. Flaud *et al.* (*13*) have obtained ν_1/ν_3 term values for $J \leq 23$. However, the highest term value $E_{\max}(J)$ (which we use as energy zero in Fig. 4b) has been determined for $J = 0$ through 13, and consequently we display the experimental results for this range of J values only. The arbitrary nature of the assignment of standard quantum number labels (v_1, v_2, v_3) is demonstrated here through the fact that even though there is rather good agreement between the calculated term values of Fig. 4a and the experimentally derived values of Fig. 4b, the MORBID vibrational assignment often differs from that given by Flaud *et al.* (*13*).

V. ANALYSIS

As already discussed in some detail in Ref. (*8*), we can transform the MORBID eigenfunctions (and, consequently, all linear combinations of MORBID eigenfunctions) to be linear combinations of "primitive" basis functions $|n_1 n_3\rangle|v_2, |k|\rangle|J, k, M\rangle$:

$$\psi(r_1, r_3, \rho, \theta, \phi, \chi) = \sum_{n_1,n_3,v_2} \sum_{k=-J}^{J} c_{n_1,n_3,v_2,k} |n_1, n_3\rangle|v_2, |k|\rangle|J, k, M\rangle. \quad (1)$$

The wavefunction depends on the internuclear distances r_j, $j = 1$ or 3, where each r_j is defined as the distance between the "outer" nucleus j and the "center" nucleus 2, on the bending coordinate ρ defined in Ref. (*9*), and on the three Euler angles θ, ϕ, and χ describing the molecular rotation (*9*). In Eq. (1), $|J, k, M\rangle$ is an eigenfunction for a rigid symmetric top, the function $|v_2, |k|\rangle$ is defined in Section II, and

$$|n_1 n_3\rangle = \Phi_{n_1}^{(1)}(r_1)\Phi_{n_3}^{(3)}(r_3) \quad (2)$$

is the product of two Morse oscillator eigenfunctions $\Phi_{n_j}^{(j)}(r_j)$, one for each internuclear distance [see Ref. (*9*)].

In the present work, we are concerned with wavefunctions given by Eq. (1). These functions are either MORBID eigenfunctions, in which case the expansion coefficients $c_{n_1,n_3,v_2,k}$ of Eq. (1) are obtained directly as eigenvector coefficients from the MORBID program, or they are linear combinations of MORBID eigenfunctions [as, for example, the primitive cluster wavefunctions or localized wavefunctions discussed extensively in Ref. (*8*)], in which case the expansion coefficients are linear combinations of MORBID eigenvector coefficients.

As the first step in analyzing the wavefunctions, we introduce the primitive cluster states already discussed in Section III. The four basis functions for a given cluster always span the reducible representation $A_1 + A_2 + B_1 + B_2$ of the molecular symmetry group $C_{2v}(M)$ (*14*), and we let $|A_1\rangle$, $|A_2\rangle$, $|B_1\rangle$, and $|B_2\rangle$ denote the four sym-

metrized MORBID eigenfunctions for a cluster. Equation (17) of Ref. (*8*) now shows that we can choose the first primitive cluster state as

$$|\text{PCS } 1\rangle = \tfrac{1}{2}(|A_1\rangle + |B_2\rangle + |B_1\rangle + |A_2\rangle). \tag{3}$$

We can now obtain the other three primitive cluster states by letting the symmetry operations of the group $C_{2v}(M)$ act on the function $|\text{PCS } 1\rangle$. For example, when the operation (13) is the interchange of the two hydrogen nuclei (see Fig. 1), we obtain the second primitive cluster state as

$$|\text{PCS } 2\rangle = (13)|\text{PCS } 1\rangle = \tfrac{1}{2}(|A_1\rangle - |B_2\rangle - |B_1\rangle + |A_2\rangle), \tag{4}$$

where the effect of (13) on the MORBID eigenfunctions can be determined from the character table of $C_{2v}(M)$ given as Table A-4 of Ref. (*14*). The third and fourth primitive cluster states, $|\text{PCS } 3\rangle$ and $|\text{PCS } 4\rangle$, can be straightforwardly obtained by letting the spatial inversion E^* and the combined operation $(13)^* = (13)E^*$, respectively, act on the function $|\text{PCS } 1\rangle$. Since there are small energy splittings between the individual cluster states, the primitive cluster functions are approximate eigenfunctions for the rotation–vibration Hamiltonian. Only in the case that the four cluster states were exactly degenerate, would these functions be exact eigenfunctions.

On the basis of k probabilities p_k given by

$$p_k = \sum_{n_1,n_3,v_2} |c_{n_1,n_3,v_2,k}|^2 \tag{5}$$

[see also Ref. (*17*)] we can identify the so-called localization axes predicted by semiclassical theory. These axes are discussed extensively in Ref. (*8*).

Finally, we determine the probability density in (r_1, r_3) space for the wavefunctions given in Eq. (1). This probability density is given by

$$\mathcal{P}(r_1, r_3) = \int_0^{\pi} d\rho \int_0^{\pi} \sin\theta d\theta \int_0^{2\pi} d\phi \int_0^{2\pi} d\chi |\psi(r_1, r_3, \rho, \theta, \phi, \chi)|^2. \tag{6}$$

The quantity

$$dP = \mathcal{P}(r_1, r_3) dr_1 dr_3 \tag{7}$$

is the differential probability of finding the molecule described by the wavefunction $\psi(r_1, r_3, \rho, \theta, \phi, \chi)$ in the volume element $dr_1 dr_3$ of (r_1, r_3) space for arbitrary values of the remaining coordinates ρ, θ, ϕ, and χ. Owing to the orthonormality of the functions $|v_2, |k|\rangle$ and $|J, k, M\rangle$, we derive

$$\mathcal{P}(r_1, r_3) = \sum_{k=-J}^{J} \sum_{v_2} \sum_{n_1,n_3} \sum_{n_1',n_3'} c^*_{n_1',n_3',v_2,k} c_{n_1,n_3,v_2,k} \Phi^{(1)}_{n_1'}(r_1)^* \Phi^{(3)}_{n_3'}(r_3)^* \Phi^{(1)}_{n_1}(r_1) \Phi^{(3)}_{n_3}(r_3). \tag{8}$$

The functions $\Phi^{(j)}_{n_j}(r_j)$, $j = 1$ or 3, can be expressed in analytical form (see, for example, Efremov (*18*) or Ref. (*11*)) so that when we have obtained the expansion coefficients $c_{n_1,n_3,v_2,k}$ from a MORBID calculation, we can straightforwardly compute values of the function $\mathcal{P}(r_1, r_3)$.

We have further found it useful to calculate the quantum mechanical expectation values of the internuclear distances r_1 and r_3 (Fig. 1). These expectation values (the "average bond lengths") are given by

$$\overline{r_j} = \int_0^\infty dr_1 \int_0^\infty dr_3 r_j \mathcal{P}(r_1, r_3), \tag{9}$$

$j = 1$ or 3. The integrals in Eq. (9) are calculated numerically using Simpson's rule (*19*).

(a) k Probabilities

We now subject the cluster wavefunctions in the top cluster of the ν_1/ν_3 state of $H_2{}^{80}Se$ to the rotational analysis employed in Ref. (*8*) for the cluster wavefunctions in the vibrational ground state of this molecule. Initially we use Eq. (3) to obtain the primitive cluster function $|\text{PCS } 1\rangle$ for the cluster in question, and we calculate the k probabilities for this function from Eq. (5). The primitive cluster wavefunction $|\text{PCS } 1\rangle$ is now rotated through an angle φ around the molecule-fixed x-axis (the axis perpendicular to the molecular plane), and the function resulting from this rotation is denoted as $R_x^{(\varphi)}|\text{PCS } 1\rangle$. We determine the angle φ such that the rotated function $R_x^{(\varphi)}|\text{PCS } 1\rangle$ has the "sharpest" possible k distribution; i.e., by varying φ we aim at obtaining a rotated function $R_x^{(\varphi)}|\text{PCS } 1\rangle$ which, for one particular k value, k_{Local} say, has a k probability $p_{k_{\text{Local}}} \approx 1$, and k probabilities $p_k \approx 0$ for $k \neq k_{\text{Local}}$.

Figure 5 presents k probabilities calculated for the cluster at highest energy in the ν_1/ν_3 state of $H_2{}^{80}Se$ at $J = 20$, 30, and 40, respectively. The empty circles show the k probabilities for the function $|\text{PCS } 1\rangle$; $k\hbar$ is the projection of the total angular momentum on the molecule-fixed z-axis. The filled circles show k probabilities for the rotated function $R_x^{(\varphi)}|\text{PCS } 1\rangle$. As for the vibrational ground state (*3, 8*), we observe from Fig. 5 that the primitive cluster wavefunctions behave essentially as the eigenfunctions of a rigid symmetric top, but the defined projection of the total angular momentum is found along an axis A that lies in the molecular plane and forms an angle φ with the molecule-fixed z-axis (see Fig. 1). We used the values $\varphi = 36°$ for $J = 20$, $\varphi = 41°$ for $J = 30$, and $\varphi = 43°$ for $J = 40$. These values were chosen such that they gave the "sharpest" k distribution in the sense defined above. Hence the localization axes found in the ν_1/ν_3 state are almost coincident with those found for the vibrational ground state (*3, 8*); they lie approximately along the H–Se bonds. We note that the angle φ approaches the limiting value 45° for very large J values exactly as was found for the vibrational ground state (*3, 8*). However, for a given J value φ is always closer to 45° in the ν_1/ν_3 state than in the vibrational ground state; i.e., in the ν_1/ν_3 state, it approaches the limiting value faster as J increases. This means that in the ν_1/ν_3 state, the cluster formation occurs at lower J values than in the vibrational ground state. For example, we calculate the "size" (the energy splitting between the highest and lowest cluster states) of the ν_1/ν_3 cluster at highest energy as 0.027 cm^{-1} ($\approx$800 MHz) at $J = 20$. For the vibrational ground state, the size of the cluster at highest energy is found experimentally to be approximately 300 GHz at $J = 20$ (*1*).

(b) Probability Density Functions

Through the k probabilities described above, we can understand the rotational motion of the molecule in the cluster states. The rotational analysis of the preceding section has shown that the "new" clusters formed in the ν_1/ν_3 state of $H_2{}^{80}Se$ through coalescence of individual ν_1 and ν_3 energy levels exhibit essentially the same type of rotational motion as we have found for cluster states in isolated vibrational states: the cluster wavefunction has a defined projection of the total angular momentum along

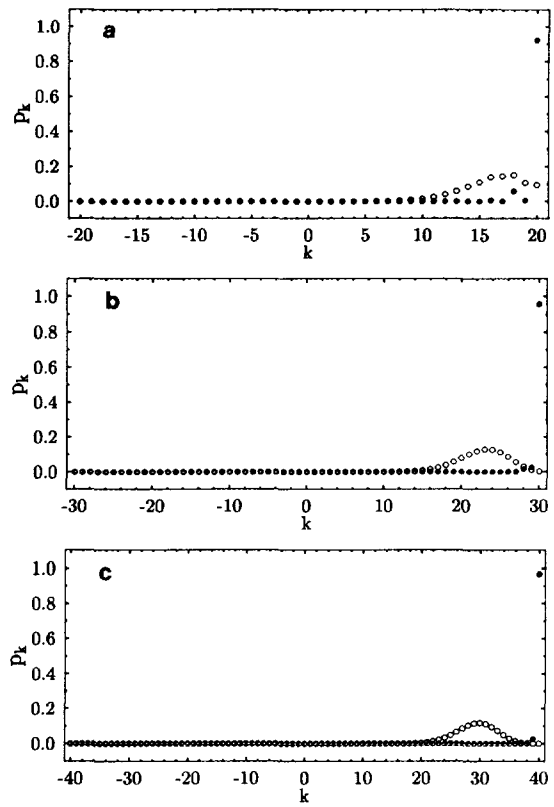

FIG. 5. The k distributions of the primitive cluster state $|\text{PCS } 1\rangle$ in the top ν_1/ν_3 cluster for $H_2{}^{80}Se$. Distributions are shown for (a) $J = 20$, (b) $J = 30$, and (c) $J = 40$. The empty circles show the k probabilities p_k for the localized wavefunction $|\text{PCS } 1\rangle$ and the filled circles show the analogous k probabilities for the function $R_x^{(\varphi)}|\text{PCS } 1\rangle$ obtained by rotating $|\text{PCS } 1\rangle$ through an angle φ around the molecule fixed x-axis (the axis perpendicular to the molecular plane).

an axis approximately coinciding with one of the Se–H bonds. However, since the new cluster states involve a massive interaction between the ν_1 and ν_3 basis states, we expect that the molecule will carry out an unusual stretching motion in these states, and we analyze this motion here through the probability density functions $\mathcal{P}(r_1, r_3)$ defined in Eq. (6).

Figure 6 shows two rather trivial examples of probability density functions: Figs. 6a and 6b show the functions $\mathcal{P}(r_1, r_3)$ for the rotational levels $0_{0\,0}$ and $20_{20\,0}$, respectively, in the vibrational ground state of $H_2{}^{80}Se$. In both cases, we obtain a bell-shaped probability density function in qualitative agreement with predictions from harmonic oscillator theory. In particular, even though the $20_{20\,0}$ state belongs to a fourfold cluster, there is no evidence of this fact in its probability density function. The primitive cluster states formed from the MORBID eigenfunctions of the four levels $20_{20\,0}$, $20_{20\,1}$, $20_{19\,1}$, and $20_{19\,2}$ in the vibrational ground state will also have probability density functions of the type shown in Fig. 6. These primitive cluster states involve one vibrational state only, and the probability density functions $\mathcal{P}(r_1, r_3)$ for all cluster wavefunctions will be given essentially by the probability density function for the $J = 0$ level of this vibrational state. We have encountered such clusters in the

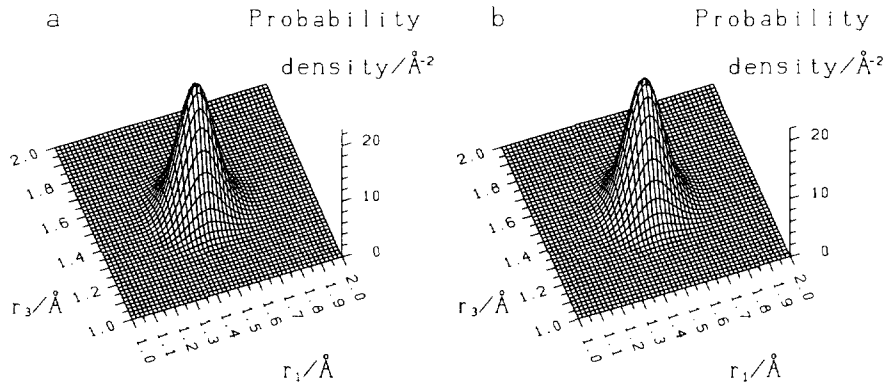

FIG. 6. Probability density functions $\mathcal{P}(r_1, r_3)$ from Eq. (6) for (a) the $J_{K_aK_c} = 0_{0\,0}$ level and (b) the $J_{K_aK_c} = 20_{20\,0}$ level in the vibrational ground state of $H_2{}^{80}Se$.

vibrational ground state (*8*) and in the ν_2 state (Section III) of H_2Se, and in the following we refer to them as Type I clusters.

If we use Eq. (9) to calculate the average values $\overline{r_j}$ of the bond lengths for any MORBID eigenfunction, we always obtain $\overline{r_1} = \overline{r_3}$. This is because the MORBID eigenfunction has a defined symmetry in the molecular symmetry group $C_{2v}(M)$ (*14*) so that its probability density function $\mathcal{P}(r_1, r_3)$ will be symmetrical under the interchange of r_1 and r_3: $\mathcal{P}(r_3, r_1) = \mathcal{P}(r_1, r_3)$. For example, for the $J = 0$ level of the vibrational ground state (Fig. 6a) we calculate $\overline{r_1} = \overline{r_3} = 1.479$ Å. However, primitive cluster states do not have defined symmetries in $C_{2v}(M)$ so their probability density functions will have $\mathcal{P}(r_3, r_1) \neq \mathcal{P}(r_1, r_3)$, leading to $\overline{r_1} \neq \overline{r_3}$. If we use Eq. (3) to construct the first primitive cluster state $|\text{PCS } 1\rangle$ in the cluster at highest energy at $J = 20$ in the vibrational ground state of $H_2{}^{80}Se$, we obtain for this state $\overline{r_1} = 1.502$ Å and $\overline{r_3} = 1.483$ Å. Hence, in the primitive cluster state $|\text{PCS } 1\rangle$ for the top cluster in the vibrational ground state at $J = 20$, the internuclear distance r_1 is lengthened by $\Delta r_1 = 0.023$ Å, and the distance r_3 is lengthened by $\Delta r_3 = 0.004$ Å, relative to the $J = 0$ level. It follows from the results of Ref. (*8*) that in the primitive cluster state $|\text{PCS } 1\rangle$ at $J = 20$, the molecule rotates around an axis A approximately coinciding with the Se–H_3 bond (see Fig. 1). The Se–H_1 bond is almost perpendicular to the A-axis, and the significant elongation of this bond ($\Delta r_1 = 0.023$ Å) relative to the $J = 0$ state is clearly due to centrifugal distortion. The elongation of the Se–H_3 bond ($\Delta r_3 = 0.004$ Å) is much smaller because this bond lies essentially along the axis of rotation.

The probability density functions for the $J = 0$ levels of the ν_1 and ν_3 vibrational states are shown in Fig. 7. These functions are in qualitative agreement with predictions from harmonic oscillator theory. The MORBID eigenfunction $|\nu_1; 0_{0\,0}\rangle$ for the $J = 0$ level of the ν_1 vibrational state would clearly be rather well approximated by a product of two harmonic oscillator functions, one having $v_1 = 1$ and depending on a normal coordinate Q_1 proportional to $(r_1 - r_1^e) + (r_3 - r_3^e)$ and the other having $v_3 = 0$ and depending on a normal coordinate Q_3 proportional to $(r_1 - r_1^e) - (r_3 - r_3^e)$. Similarly, the MORBID eigenfunction $|\nu_3; 0_{0\,0}\rangle$ for the $J = 0$ level of the ν_3 vibrational state would be well approximated by an analogous product, in which the harmonic oscillator function depending on Q_1 has $v_1 = 0$ and that depending on Q_3 has $v_3 = 1$. We introduce here two *local mode* wavefunctions (*20*) given by

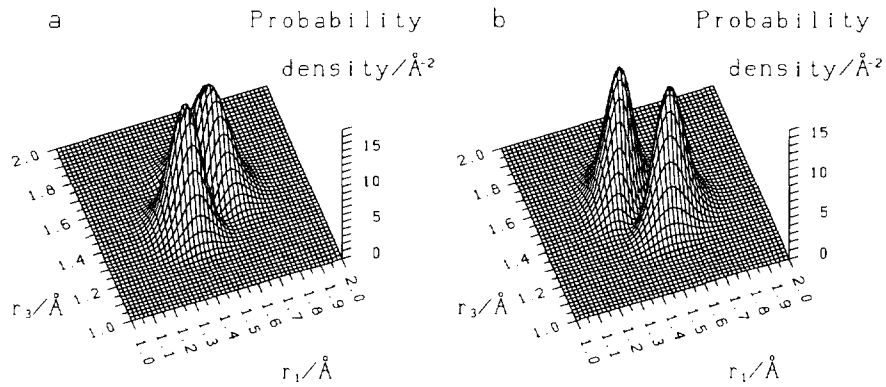

FIG. 7. Probability density functions $\mathcal{P}(r_1, r_3)$ from Eq. (6) for (a) the $J_{K_aK_c} = 0_{00}$ level in the ν_1 vibrational state and (b) the $J_{K_aK_c} = 0_{00}$ level in the ν_3 vibrational state of $H_2{}^{80}Se$.

$$|\psi_\pm\rangle = \frac{1}{\sqrt{2}}(|\nu_1; 0_{0\,0}\rangle \pm |\nu_3; 0_{0\,0}\rangle). \tag{10}$$

The probability density functions for these two functions are given in Fig. 8. The figure shows that the wavefunction $|\psi_+\rangle$ has one node in the r_3 direction and no nodes in the r_1 direction. Consequently, it represents a localized excitation of the Se–H_3 stretching motion. The wavefunction $|\psi_-\rangle$ has one node in the r_1 direction and no nodes in the r_3 direction so that it represents a localized excitation of the Se–H_1 stretching motion. It should be noted that the functions $|\psi_+\rangle$ and $|\psi_-\rangle$ are not eigenfunctions of the rotation–vibration Hamiltonian. We show their probability density functions here in order to facilitate the discussion of the stretching motion in the ν_1/ν_3 cluster states given below.

We can now proceed to study the probability density functions for the ν_1/ν_3 cluster states. Figure 9 shows the probability density functions for the two MORBID eigenfunctions with symmetries A_1 and A_2, respectively, belonging to the cluster at highest energy in the ν_1/ν_3 state at $J = 20$. The two remaining cluster eigenfunctions (with

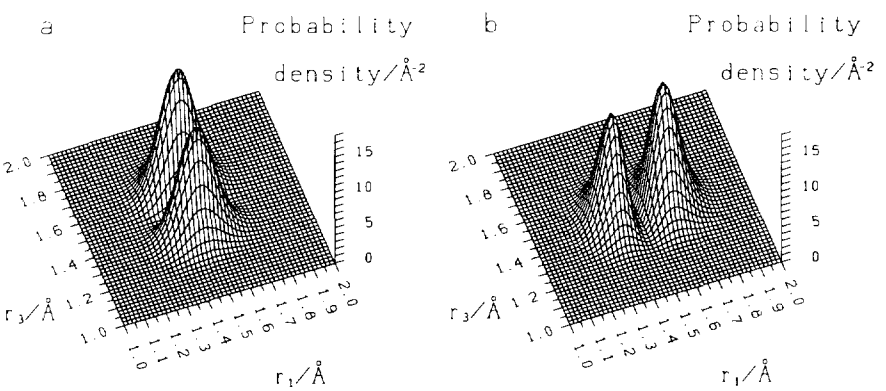

FIG. 8. Probability density functions $\mathcal{P}(r_1, r_3)$ from Eq. (6) for (a) the wavefunction $|\psi_+\rangle$ and (b) the wavefunction $|\psi_-\rangle$ given by Eq. (10). The probability density functions are calculated for $H_2{}^{80}Se$.

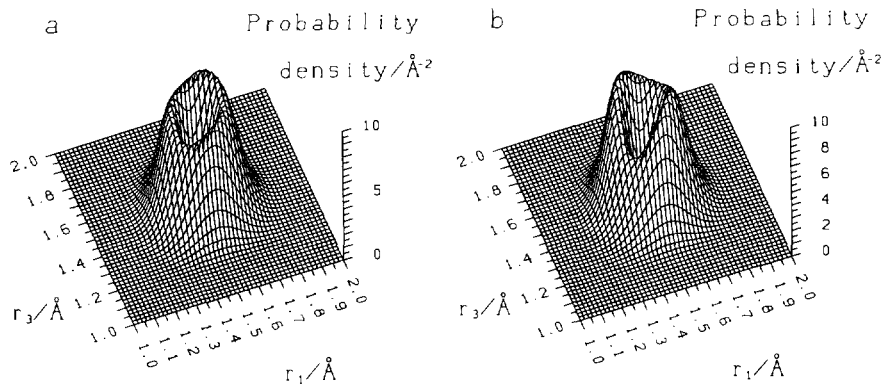

FIG. 9. Probability density functions $\mathcal{P}(r_1, r_3)$ from Eq. (6) for (a) the MORBID eigenfunction with symmetry A_1 and (b) the MORBID eigenfunction with symmetry A_2 belonging to the cluster at highest energy in the ν_1/ν_3 state at $J = 20$ for $H_2{}^{80}Se$.

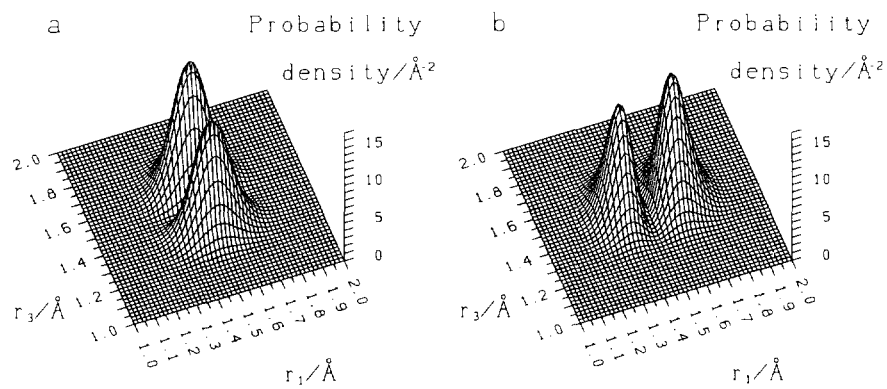

FIG. 10. Probability density functions $\mathcal{P}(r_1, r_3)$ from Eq. (6) for (a) the first primitive cluster state $|\text{PCS } 1\rangle$ and (b) the second primitive cluster state $|\text{PCS } 2\rangle$ belonging to the cluster at highest energy in the ν_1/ν_3 state at $J = 20$ for $H_2{}^{80}Se$.

symmetries B_1 and B_2, respectively) produce two probability density functions essentially indistinguishable from those shown in the figure. Owing to the massive interaction between ν_1 and ν_3 basis states found for these cluster wavefunctions, the probability density functions differ qualitatively from those found in the ν_1 and ν_3 states for $J = 0$ (Fig. 7). The "volcano" structures of Fig. 9 arise as superpositions of the probability density functions of Figs. 7a and 7b.

We now use Eqs. (3) and (4) to construct the first and second primitive cluster states, $|\text{PCS } 1\rangle$ and $|\text{PCS } 2\rangle$, in the ν_1/ν_3 state at $J = 20$. Figure 10 shows the probability density functions for these two wavefunctions. Obviously these two probability density functions are indistinguishable from those given for the local mode wavefunctions $|\psi_+\rangle$ and $|\psi_-\rangle$ in Fig. 8, and we conclude that two primitive cluster states show local mode behavior. The wavefunction $|\text{PCS } 1\rangle$ describes a localized excitation of the Se–H_3 stretching motion and the wavefunction $|\text{PCS } 2\rangle$ a localized excitation of the Se–H_1 stretching motion. We can obtain the third and fourth primitive cluster states, $|\text{PCS } 3\rangle$ and $|\text{PCS } 4\rangle$, by letting the spatial inversion E^* (*14*) act on $|\text{PCS } 1\rangle$ and $|\text{PCS } 2\rangle$, respectively. That is, $|\text{PCS } 3\rangle = E^*|\text{PCS } 1\rangle$ and $|\text{PCS } 4\rangle$

$= E^*|\text{PCS } 2\rangle$. It can be shown that $|\text{PCS } 3\rangle$ will yield exactly the same probability density function as $|\text{PCS } 1\rangle$, and $|\text{PCS } 4\rangle$ will yield exactly the same probability density function as $|\text{PCS } 2\rangle$. Hence $|\text{PCS } 3\rangle$ describes a localized excitation of the Se–H_3 stretching motion and the wavefunction $|\text{PCS } 4\rangle$ a localized excitation of the Se–H_1 stretching motion.

Since the energy splittings between the individual cluster states are small, the primitive cluster wavefunctions are good approximations for the rotation–vibration eigenfunctions. The primitive cluster wavefunctions thus constitute near-eigenstates of the rotation–vibration Hamiltonian in which the molecule exhibits local mode behavior in that the vibrational excitation is localized at specific bonds (*20*). Conventional local mode theory (*20*), which normally neglects molecular rotation entirely, expects this phenomenon to be brought about by vibrational excitation so that it will be found for highly excited stretching states only. In the present case, the local mode behavior arises through rotation–vibration interaction so that, in a sense, it is caused by rotational excitation.

The rotational analysis of the primitive cluster states belonging to the ν_1/ν_3 vibrational state (see above) showed that in the first primitive cluster state $|\text{PCS } 1\rangle$, the molecule rotates around the A-axis which lies approximately along the Se–H_3 bond (see Fig. 2). The vibrational analysis of the present section now shows the excitation of the stretching vibration to be localized in this bond. Consequently, if we use the primitive cluster states to describe the vibrational motion associated with the fourfold energy clusters in the ν_1/ν_3 vibrational state, we arrive at the following simple picture: the stretching excitation is localized in one of the bonds, and the molecule rotates around this bond. We can illustrate this further by considering the average bond length values in the ν_1/ν_3 cluster states. For the local mode function $|\psi_+\rangle$ [Eq. (10)], which represents a localized excitation of the Se–H_3 stretching motion, we calculate $\overline{r_1}$ = 1.479 Å and $\overline{r_3}$ = 1.515 Å. For the $J = 0$ level of the vibrational ground state, we calculated $\overline{r_1} = \overline{r_3}$ = 1.479 Å (see above). Hence for the wavefunction $|\psi_+\rangle$, $\overline{r_1}$ is unchanged relative to the vibrational ground state, but $\overline{r_3}$ is increased by 0.036 Å due to the vibrational excitation. For the first primitive cluster state $|\text{PCS } 1\rangle$ belonging to the top cluster in the ν_1/ν_3 vibrational state at $J = 20$, we obtain $\overline{r_1}$ = 1.504 Å and $\overline{r_3}$ = 1.517 Å. Relative to the average bond lengths found for the wavefunction $|\psi_+\rangle$, the internuclear distance r_1 is lengthened by Δr_1 = 0.025 Å, and the distance r_3 is lengthened by Δr_3 = 0.002 Å. These results are almost equal to the elongations of $(\Delta r_1, \Delta r_3)$ = (0.023 Å, 0.004 Å) determined for the first primitive cluster state $|\text{PCS } 1\rangle$ for the cluster at highest energy in the vibrational ground state at $J = 20$ relative to the $J = 0$ level of the vibrational ground state. Again, we observe that through rotational excitation to $J = 20$, the Se–H_1 bond (r_1), which is approximately perpendicular to the axis of rotation, is significantly lengthened due to centrifugal distortion, whereas the Se–H_3 bond (r_3), which lies along the rotation axis, is affected very little. The average bond lengths calculated in the present work are summarized in Table I.

Through the analysis reported in the present section, we have seen that for the primitive cluster wavefunctions belonging to the clusters at highest energy in the ν_1/ν_3 vibrational state at moderate J values, there are two possibilities for the probability density function $\mathcal{P}(r_1, r_3)$; these two possibilities are given in Figs. 10a and 10b, respectively. A primitive cluster wavefunction can either describe a localized excitation of the Se–H_3 stretching motion (Fig. 10a) or a localized excitation of the Se–H_1 stretching motion (Fig. 10b). In order to form a cluster of this type, we need two vibrational states of different symmetry, in the present case the two states ν_1 and ν_3,

TABLE I

Average Bond Length Values Calculated from Eq. (9) for Rotation–Vibration States of $H_2{}^{80}Se$

	$J = 0$		$J = 20^a$			
	$\overline{r_1}$/Å	$\overline{r_3}$/Å	$\overline{r_1}$/Å	$\overline{r_3}$/Å	$\Delta\overline{r_1}^b$/Å	$\Delta\overline{r_3}^b$/Å
V. g. s.[c]	1.479	1.479	1.502	1.483	0.023	0.004
ν_1/ν_3	1.479	1.515	1.504	1.517	0.025	0.002

[a] Average bond lengths for the first primitive cluster function |PCS 1⟩ in the "top" cluster.

[b] $\Delta\overline{r_j} = \overline{r_j}(J = 20) - \overline{r_j}(J = 0)$.

[c] Vibrational ground state.

and the fourfold clusters will be formed through coalescence of levels belonging to these two vibrational states. Obviously, the rotation–vibration energy spectrum of H_2Se contains at least two different types of clusters: the Type I clusters which we have encountered in the vibrational ground state and in the ν_2 and $2\nu_2$ vibrational states, and the new type (which we shall call Type II) found in the ν_1/ν_3 vibrational state.

With further rotational excitation, the vibrational motion in the cluster states belonging to the clusters at highest energy in the ν_1/ν_3 vibrational state becomes more complicated. Since the cluster approaches an avoided crossing with the top cluster from the $2\nu_2$ state (Fig. 3), the contribution to the eigenstates from the $2\nu_2$ basis states becomes increasingly larger. We show in Fig. 11 the probability density functions for the two MORBID eigenfunctions with symmetries A_1 and A_2, respectively, belonging to the cluster at highest energy in the ν_1/ν_3 state at $J = 30$. The effect of the increasing contribution from the $2\nu_2$ basis states is to fill the "volcano crater" seen in Fig. 9. Figure 12 shows the probability density functions for the two primitive cluster states |PCS 1⟩ and |PCS 2⟩ constructed from Eqs. (3) and (4) at $J = 30$. The probability density functions retain their local mode character, but it is obvious from Fig. 12b that the admixture of $2\nu_2$ probability starts filling the "canyon" between the two local mode maxima. The increasing interaction with $2\nu_2$ does not, however, affect the rotational localization of the wavefunctions.

VI. DISCUSSION

In our previous papers on the cluster formation in H_2Se (*1–3, 8*) we were concerned with Type I clusters. They arise within one particular vibrational state. We have encountered these clusters in the vibrational ground state and in the ν_2 vibrational state. They are also found in the $2\nu_2$ state where, however, they may be distorted through interactions with ν_1 and ν_3. Type I clusters result from the centrifugal distortion of the molecule which causes the effective A and B constants to become equal as J increases. As a consequence, with increasing J the a-axis of the molecule (the z-axis in Fig. 2) loses its stability as a quantization axis, and two new stable axes of precession appear, leading to the formation of fourfold energy clusters. This phenomenon is discussed in detail in Ref. (*1*).

The formation of Type II clusters in the ν_1 and ν_3 vibrational states is primarily caused by the interaction between these states. In this case, the stability of the a-axis

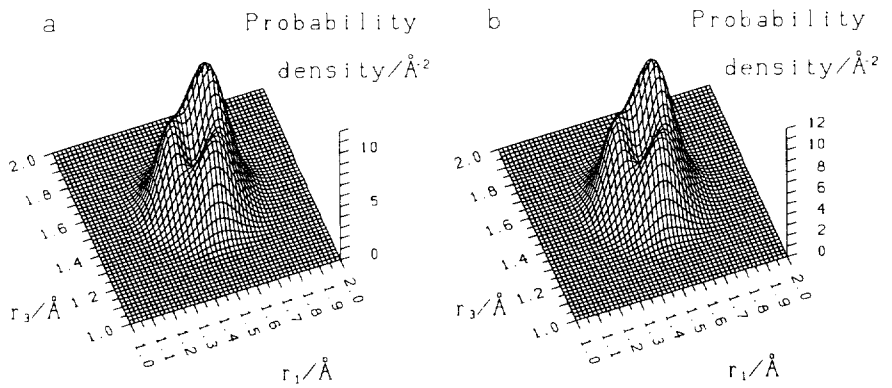

FIG. 11. Probability density functions $\mathcal{P}(r_1, r_3)$ from Eq. (6) for (a) the MORBID eigenfunction with symmetry A_1 and (b) the MORBID eigenfunction with symmetry A_2 belonging to the cluster at highest energy in the ν_1/ν_3 state at $J = 30$ for $H_2{}^{80}Se$.

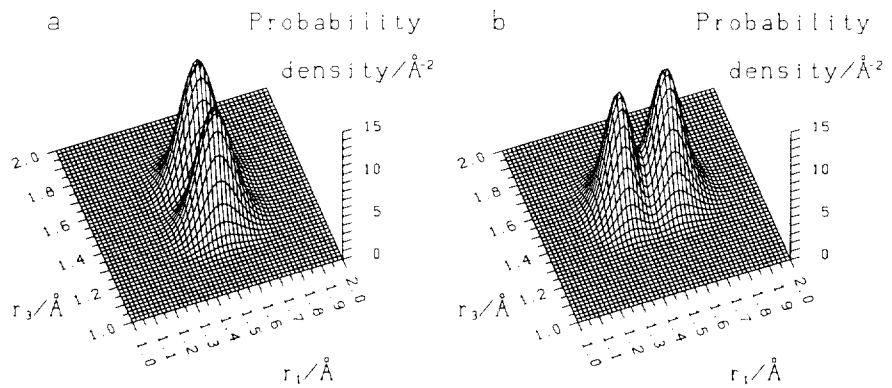

FIG. 12. Probability density functions $\mathcal{P}(r_1, r_3)$ from Eq. (6) for (a) the first primitive cluster state $|\text{PCS } 1\rangle$ and (b) the second primitive cluster state $|\text{PCS } 2\rangle$ belonging to the cluster at highest energy in the ν_1/ν_3 state at $J = 30$ for $H_2{}^{80}Se$.

is changed through the excitation of localized vibrations in the molecule. When the stretching motion of one bond is excited, the moments of inertia will change so that the principal axis with the smallest moment of inertia will lie along this bond. In classical terms, clockwise and anticlockwise rotations around this axis can take place, and there will exist two equivalent situations in which the other bond is excited, and clockwise and anticlockwise rotations around this bond occur. In total, there will be four classical trajectories with the same energy, and they correspond to the fourfold clusters which we have determined through our quantum mechanical calculation.

The cluster formation process can be understood through rotational energy surface analyses (*21–23*). In this semiclassical approach, the cluster structure is explained through the analysis of the topology of the so-called rotational energy surface for an isolated vibrational state or, in the case of interacting vibrational states, through the analysis of the topology of multiple rotational surfaces, one for each vibrational state. It was shown in Ref. (*1*) that the Type I clusters in the vibrational ground state of H_2Se can be classified as consequences of a C_{2v} critical phenomenon or a bifurcation on the rotational energy surface (*21*). We show here that the Type II clusters also originate in the C_{2v} critical phenomenon, however, the critical phenomenon is caused

to a large extent by the interaction of the ν_1 and ν_3 vibrational states. The starting point for this analysis is an effective (Watson-type) Hamiltonian which describes two vibrational states ν_1 and ν_3 coupled through Coriolis-type resonances. The parameters for this Hamiltonian are taken from the recent work of Flaud *et al.* (*13*). In the next step, we substitute the angular momentum operators $\hat{J}_x$, $\hat{J}_y$, and $\hat{J}_z$ in the effective Hamiltonian by classical values. We use standard spherical coordinates (J, θ, ϕ) to describe the classical components of the angular momentum in the molecule-fixed coordinate system, and so we make the substitutions,

$$\hat{J}_z \rightarrow J \cos\theta, \qquad \hat{J}_x \rightarrow J \sin\theta \cos\phi, \qquad \hat{J}_y \rightarrow J \sin\theta \sin\phi. \tag{11}$$

We now proceed to solve the quantum mechanical vibrational problem (through the diagonalization of a 2×2 matrix) for integer values of J and a grid of values of (θ, ϕ). The resulting two energy solutions [taken as functions of (J, θ, ϕ)] define the two rotational surfaces. Figures 13 and 14 show the intersections of these rotational surfaces with the xz-plane for different values of J. We represent the rotational energy surfaces using the molecule-fixed axis system employed by Flaud *et al.* (*13*), which differs from the axis system used by MORBID (Fig. 1). Flaud *et al.* (*13*) use a molecule-fixed axis system chosen according to the I^r representation (*14*) so that the xz-plane is the plane of the molecule. In the calculation of the rotational surfaces shown in Fig. 13, we have neglected the "pure" centrifugal distortion constants which are responsible for the formation of fourfold clusters in the vibrational ground state. Figure 13 shows

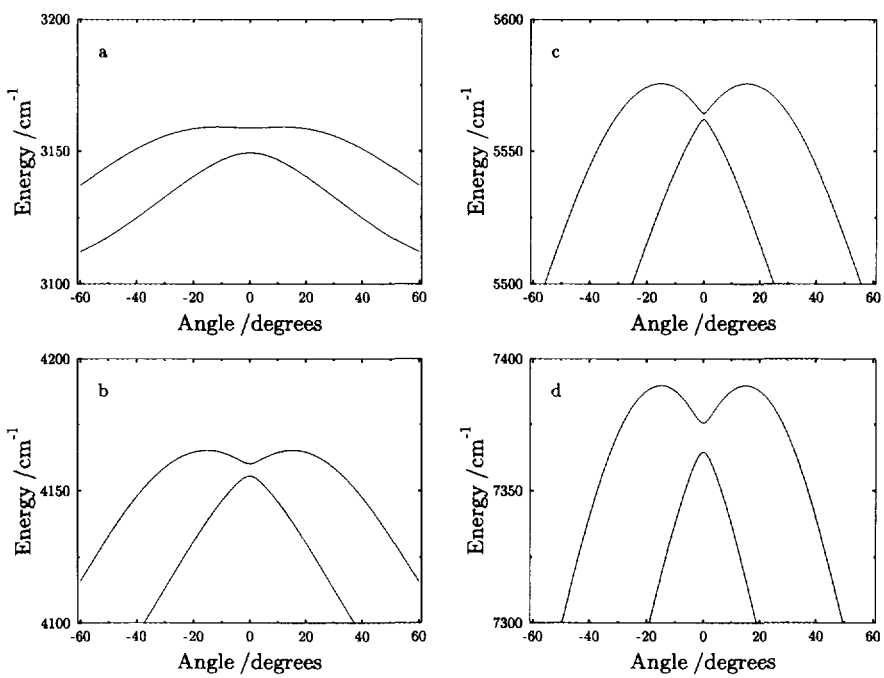

FIG. 13. Sections through the rotational energy surfaces for the ν_1/ν_3 vibrational states of $H_2{}^{80}Se$. The figures show the value of the rotational surface energy in the molecular plane as a function of the polar angle θ, i.e., the angle between the actual direction and the molecule fixed z-axis. Drawings are made for (a) $J = 10$, (b) $J = 15$, (c) $J = 20$, and (d) $J = 25$. In the calculation of the rotational energy surfaces, the "pure" centrifugal distortion constants have been set equal to zero.

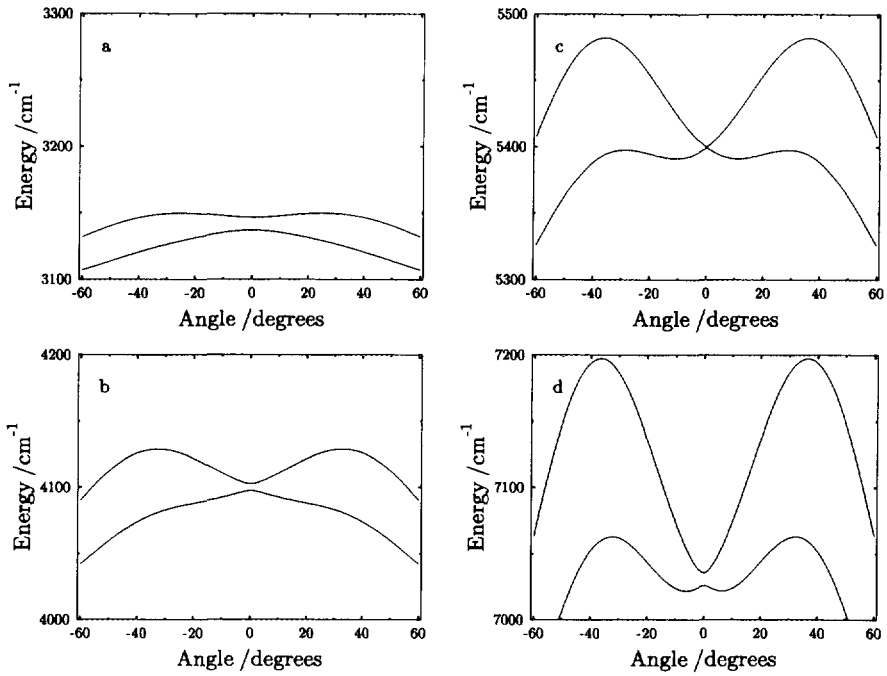

FIG. 14. Sections through the rotational energy surfaces for the ν_1/ν_3 vibrational states of $H_2{}^{80}Se$. The figures show the value of the rotational surface energy in the molecular plane as a function of the polar angle θ, i.e., the angle between the actual direction and the molecule fixed z-axis. Drawings are made for (a) $J = 10$, (b) $J = 15$, (c) $J = 20$, and (d) $J = 25$. In the calculation of the rotational energy surfaces, all centrifugal distortion effects have been taken into account.

sections of the rotational surfaces for $J = 10$, 15, 20, and 25, respectively. We see how the topology of the rotational surfaces changes with rotational excitation. Even in the approximation where the centrifugal distortion terms are neglected in the Hamiltonian (Fig. 13), four maxima are formed on the "outer" rotational energy surface. Two of these maxima are visible in Fig. 13 and the existence of the remaining two follows from the symmetry of the rotational surface. At $J = 20$ the two rotational surfaces exhibit an avoided crossing, a phenomenon referred to as a diabolic point (*22, 23*). When we include all centrifugal distortion terms in the calculation of the rotational surfaces (Fig. 14) the maxima become more pronounced. The four maxima can be associated with the appearance of fourfold clusters in the rovibrational energy spectrum. We do not give here a complete analysis of the rotational energy surface dynamics. We note, however, that Fig. 14 shows that with increasing J, θ is predicted to approach the limiting value 45°. This is in perfect agreement with the results of the quantum mechanical analysis given above.

In the present work, we have calculated the rotation–vibration energy level spectra of $H_2{}^{80}Se$ in the ν_1, ν_2, ν_3, and $2\nu_2$ vibrational states using the MORBID Hamiltonian and computer program (*9–11*). As input data for these calculations, we used a potential energy surface recently determined from experimental data with the MORBID approach (*8*). We find that in all of the vibrational states considered, fourfold rovibrational energy clusters are formed when J increases. The cluster formation in the ν_2 and $2\nu_2$ vibrational states is found to involve the centrifugal distortion mechanism already

discussed in Ref. (*8*) for the vibrational ground state (with the slight complication that the cluster pattern in the $2\nu_2$ vibrational state is sometimes distorted due to local interactions with ν_1 and ν_3). For the ν_1/ν_3 interacting vibrational states, however, doublets of ν_1 rovibrational states will blend with doublets of ν_3 rovibrational states giving rise to a new type of fourfold cluster. The wavefunctions corresponding to the cluster states are fifty-fifty mixtures of ν_1 and ν_3 basis states. If we choose to describe these new fourfold clusters using the wavefunctions for the primitive cluster states suggested by semiclassical theory, we can offer a simple description of the molecular motion in a cluster state: The stretching excitation is localized in one of the bonds, and the molecule rotates around this bond. The other bond, whose stretching motion is not excited, is lengthened due to centrifugal distortion.

The next logical step would clearly be to verify experimentally the existence of the new cluster type described here for the ν_1/ν_3 state. The most recent experimental work on the fundamental levels of H_2Se is that by Flaud *et al.* (*13*). In Figs. 2 and 4 we compare the calculated term values from the present work with their experimentally derived term values for the ν_2 state and the $\nu_1/\nu_3/2\nu_2$ state, respectively. The figures show that there is good agreement between the available experimental term values and our calculated values. However, in the ν_1/ν_3 vibrational state, the energy structure in the upper part of the J multiplets (Fig. 4) has been experimentally determined for $J \leqslant 13$ only. An experimental verification of the cluster structure shown in Fig. 4a requires the measurement of transitions to the high K states up to $J \approx 20$. In order to determine whether this would be feasible in spectra with high values of (pressure) $\times$ (absorption path length), we are presently using the MORBID intensity program (*24*) to simulate high J, high K spectra on the basis of our fitted potential energy function (*8*) and the ab initio dipole moment surface from Ref. (*25*).

ACKNOWLEDGMENTS

This work was supported by the Deutsche Forschungsgemeinschaft (through Grant Je 144/2-3) and by the Fonds der Chemischen Industrie. P.J. acknowledges further support from the Dr. Otto Röhm Gedächtnisstiftung and from the Fritz Thyssen-Stiftung. The present work has only been possible through the use of two supercomputers recently made available to us by the State of Hessen: the Siemens/Nixdorf S400/40 installation at the Technical University Darmstadt and the Siemens/Nixdorf S100/10 installation at the Justus Liebig University Giessen. The major part of the calculations reported here was carried out on these installations, and we are grateful for generous allotments of computer time. We thank N. Conrad and J. Preusser for assistance with the numerical calculations. I.N.K. is grateful to the Institute of Physical Chemistry at the Justus Liebig University Giessen, and particularly to B.P. Winnewisser and M. Winnewisser, for hospitality. We thank P. R. Bunker, B. I. Zhilinskii, and B. P. Winnewisser for critically reading the manuscript and suggesting alternatives, and H. Bürger and J.-M. Flaud for communicating their results prior to publication.

RECEIVED: April 1, 1993

REFERENCES

1. I. N. KOZIN, S. P. BELOV, O. L. POLYANSKY, AND M. YU. TRETYAKOV, *J. Mol. Spectrosc.* **152,** 13–28 (1992).
2. I. N. KOZIN, O. L. POLYANSKY, S. I. PRIPOLZIN, AND V. L. VAKS, *J. Mol. Spectrosc.* **156,** 504–506 (1992).
3. I. N. KOZIN, S. KLEE, P. JENSEN, O. L. POLYANSKY, AND I. M. PAVLICHENKOV, *J. Mol. Spectrosc.* **158,** 409–422 (1993).
4. B. I. ZHILINSKII AND I. M. PAVLICHENKOV, *Opt. Spectrosc. (USSR)* **64,** 688–690 (1988). [In Russian]
5. J. MAKAREWICZ AND J. PYKA, *Mol. Phys.* **68,** 107–127 (1989).
6. J. MAKAREWICZ, *Mol. Phys.* **69,** 903–921 (1990).

7. J. PYKA, *Mol. Phys.* **70,** 547–561 (1990).
8. P. JENSEN AND I. N. KOZIN, *J. Mol. Spectrosc.*, in press.
9. P. JENSEN, *J. Mol. Spectrosc.* **128,** 478–501 (1988).
10. P. JENSEN, *J. Chem. Soc. Faraday Trans. 2* **84,** 1315–1340 (1988).
11. P. JENSEN, *in* "Methods in Computational Molecular Physics" (S. Wilson and G. H. F. Diercksen, Eds.), Plenum Press, New York, 1992.
12. P. JENSEN, *Comp. Phys. Rep.* **1,** 1–55 (1983).
13. J.-M. FLAUD, C. CAMY-PEYRET, H. BÜRGER, AND H. WILLNER, *J. Mol. Spectrosc.* **161,** 157–169 (1993).
14. P. R. BUNKER, "Molecular Symmetry and Spectroscopy," Academic Press, London, 1979.
15. D. PAPOUŠEK AND M. R. ALIEV, "Molecular Vibrational-Rotational Spectra," Elsevier, Amsterdam, 1982.
16. F. W. BIRSS, *Mol. Phys.* **31,** 491–500 (1976).
17. S. G. LARSEN AND S. BRODERSEN, *J. Mol. Spectrosc.* **157,** 220–236 (1993).
18. YU. S. EFREMOV, *Opt. Spectrosc. (USSR)* **43,** 693–694 (1977). [In English]
19. H. MARGENEAU AND G. M. MURPHY, "The Mathematics of Physics and Chemistry," Van Nostrand-Reinhold, Princeton, NJ, 1956.
20. I. M. MILLS AND A. G. ROBIETTE, *Mol. Phys.* **56,** 743–765 (1985).
21. I. M. PAVLICHENKOV AND B. I. ZHILINSKII, *Ann. Phys. (N.Y.)* **184,** 1–32 (1988).
22. V. M. KRIVTSUN, D. A. SADOVSKII, AND B. I. ZHILINSKII, *J. Mol. Spectrosc.* **139,** 126–146 (1990).
23. D. A. SADOVSKII, B. I. ZHILINSKII, J.-P. CHAMPION, AND G. PIERRE, *J. Chem. Phys.* **92,** 1523–1537 (1990).
24. P. JENSEN, *J. Mol. Spectrosc.* **132,** 429–457 (1988).
25. J. SENEKOWITSCH, A. ZILCH, S. CARTER, H.-J. WERNER, P. ROSMUS, AND P. BOTSCHWINA, *Chem. Phys.* **122,** 375–386 (1988).